MATEC Web of Conferences **32**, 05001 (2015)
DOI: 10.1051/matecconf/20153205001

Fluorescence microscope by using computational ghost imaging

Yasuhiro Mizutani[1,3], Kyuki Shibuya[2], Tetsuo Iwata[2,3], and Yasuhiro Takaya[1]

[1] *Osaka university, Department of mechanical engineering, 560-0871 Osaka Japan*
[2] *Tokushima university, Institute of technology and science, 770-8506 Tokushima Japan*
[3] *JST/ERATO Minoshima Intelligent Optical Synthesizer Project, 770-8506 Japan*

Abstract. We propose a fluorescence microscope by using the computational Ghost imaging (CGI) for observing a living cell for a long duration over an hour. There is a problem for observing a cell about light-induced bleaching for a ling-term observation. To over come the problem, we focused on an advantage of sensitivity of the CGI as second order colleration for an imaging with weak intensity excitation light. Setting for the CGI, a DMD projector was installed at an eye-piece part of a microscope and fluorescent light was detected using a bucket detector of a photo-multiplier tube. As a results, we have shown the imaging advantage of the CGI under weak light intensity, in addition, we have demonstrated to detect fluorescence images of biological samples for one day.

1 Introduction

Fluorescence-microscopic imaging is a powerful tool for analyzing in the biological field for the past decades[1]. There have been a number of reports about the microscopes in the view points of its spacial resolution, sensitivity, and usefulness. Although the spacial resolution is one of the most important objects for development of the fluorescence microscope, the sensitivity is also important problem for observing biological samples because there is light-induced bleaching. In previous works, a fluorescent molecule can emit photons of 10^5-10^6 before bleaching[2, 3]. The limitation affects for a term of the observation. Therefore, an observation method using low intensity excitation is more desirable for long-term observation.

To overcome the problem, we focused on the Ghost imaging (GI) which is a correlation based imaging by using a bucket detector instead of such a 2D detector as CCD or CMOS sensors. The GI was first described by Belinsky and Pittman for detecting entangled photons by second-order correlation[4, 5]. Then the GI using a thermal light source by using speckle has been proposed by Gatti [6]. The speckle GI have found broad application where its usefulness presents advantages over preparing the entangled photons. More recently by using a digital mirror device (DMD) projector or a spatial light modulator (SLM) for a light source which were called the computational GI (CGI), a simple optical system could be constructed and it was easy to install into the various optical systems[7, 8].

By using the GI or CGI as fluorescence-imaging methods, there is an advantage for weak intensity imaging because a sensitivity of a bucket detector is higher than 2D detectors and there is a multiplex effect[9]. There exists some literature on the fluorescence imaging using the GI or CGI. First paper of the fluorescence GI (FGI) has been proposed by Yun for detecting the entangled-photon[10]. Tanha et. al. was then reported spectral imaging by the GI [11–14]. Although the GI or CGI have demonstrated to apply to a fluorescence imaging, there was very little quantitative data on the weak intensity measurement.

In this paper, we propose a possibility to observe for weak intensity of the fluorescence by using the CGI, theoretically and experimentally. For using the fluorescence CGI (FCGI), we first give the advantage of detecting the weak intensity in the view point of the contrast-to-noise ratio and then present the fluorescence imaging of biological samples for long-term observation without photobleaching.

2 Computational Ghost imaging for fluorescent microscope

A basic configuration of the FCGI is shown in fig. 1. Random-patterned excitation lights from a DMD projector or a SLM are projected on a fluorescent staining cells. Then fluorescence signals thorough a band pass filter for cutting the excitation light are detected by a bucket detector. Finally, by analyzing a correlation between the illuminated signals and the detected signals, a fluorescence image can be detected as a 2D distribution of a correlation efficient.

The n-th signal detected by the bucket detector B_n is described as

$$B_n = \int\int I_n(x,y)T(x,y)\Omega dxdy, \qquad (1)$$

where $I_n(x,y)$ is a intensity distribution of a n-th illuminated pattern, $T(x,y)$ is a distribution of a fluorescence

Article available at http://www.matec-conferences.org or http://dx.doi.org/10.1051/matecconf/20153205001

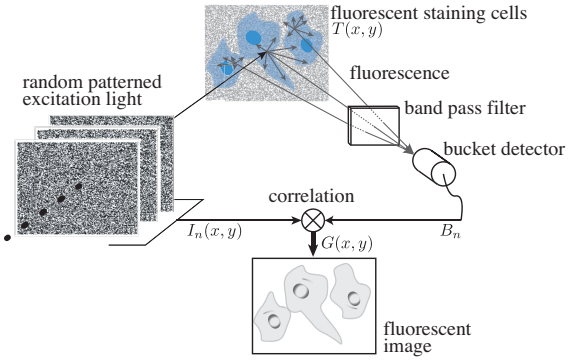

Figure 1. Basic configuration of fluorescent imaging by using computational Ghost imaging.

molecule on a sample, and Ω is detection cross section of the bucket detector. By calculating the correlation between the illuminated pattern $i_n(x, y)$ and the detected B_n, a distribution of a second-order correlation $G(x, y)$ is given by

$$G(x, y) = \langle B_n I_n(x, y)\rangle - \langle B_n\rangle\langle I_n(x, y)\rangle, \tag{2}$$

where $\langle\rangle$ is the average operator. $G(x, y)$ is proportional to the intensity of the fluorescence light, therefore, a distribution of the fluorescence intensity can be detected by the CGI.

3 Quantitative analysis for advancement of detecting weak light

We have attempted to analyze advantages of the CGI for detecting weak intensities, numerically and experimentally. We set a projected pattern and a sample of size 100 × 100 pixels. Intensity distribution of the projected pattern was generated by random numbers with the continuous uniform distribution from 0 to 1. Intensity distribution of the fluorescence sample was set as 0 or 1. We have estimated there was an electrically noise in detected signals, therefore, a detected signal with noise $e_{n,noise}$, $B_{n,noise}$, was described as

$$B_{n,noise} = B_n + e_{n,noise}. \tag{3}$$

We set a detected signal $B_{n,noise}$ instead of B_n in eq.(2). Then calculated distributions of the correlation efficiency has been derived by eq.(2).

Figures 2 shows numerical results of the fluorescent imaging. The object and calculated images of signal-to-noise ratio 0.1 are shown in fig. 2(a). In the setting object, there was non-fluorecence area with fluorescence area of size 50 × 50 pixels. For comparison between a general imaging and the proposed method, an image detected by a scanning method was also calculated uniformly. As shown in fig.2 (a), in the case of detection by the scanning method, the object can not seen and there is random noise. On the other hand, by using the CGI with 10000 measurements, the object pattern can be seen a fine image. A visibility of the CGI is better than the image of the scanning method.

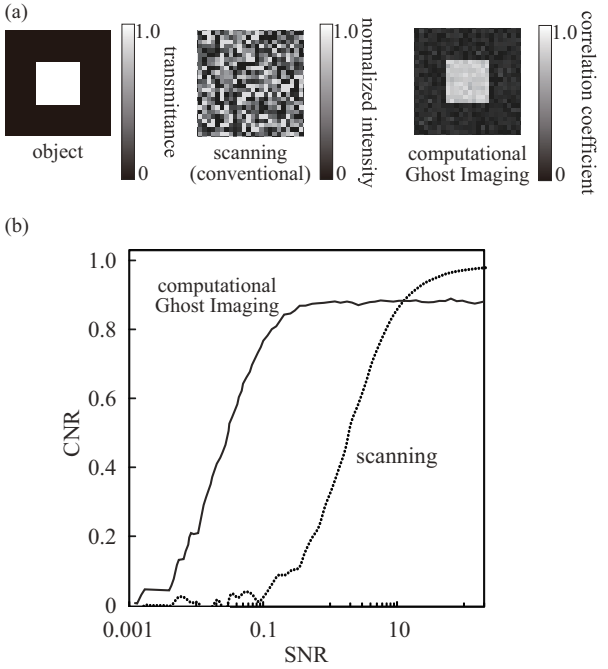

Figure 2. Numerical results of images under low SNR for comparison between conventional and proposed method. (a) setting object and calculated images with SNR = 0.10, (b) variation of image quality with SNR.

A numerical result of quantitatively analysis is shown in fig. 2(b). We used a contrast-to-noise ratio (CNR) for estimation quantitatively. The CNR is useful for comparison of image qualities and it was defined as [15]

$$CNR \equiv \frac{\langle G_1\rangle - \langle G_0\rangle}{\sqrt{\sigma_1^2 + \sigma_0^2}}, \tag{4}$$

where $\langle G_1\rangle$ and $\langle G_0\rangle$ are the average of the reconstruction values of the transmission area and masked area, respectively, and σ_1^2 and σ_0^2 are the corresponding variances. Both CNR increase with increasing SNR, leaving off at higher SNR. Moreover, the CNR of the scanning method is higher than that of the CGI at the range of the higher SNR. However, at the SNR ranges under 0.3, the CNR of the CGI is better than that of the scanning method. The most likely causes are the multiplex and the correlation effects.

Figure 3 shows the dependence of the CNR on the SNR for the experimental images.. The object consisted of a mask containing a 5 × 5 mm transmission area. The projection unit was a 2D scanning mirror (OPUS PC140015). The diameter of the scanning mirror was 1.2 mm and the scanning speed of the fast and slow axes was 13580 Hz and 1565 Hz, respectively. The light source of the optical scanner was an 18 μ W LD with a wavelength of 635 nm. To reduce the fluctuations of the illumination light from the light source, we used an exposure time of 300 ms/pattern. The illumination pattern was a 250-μm/pixel square on the object plane. The point detector was a Si PIN photodiode (Hamamatsu S5971), which detected at

100 MHz. For each method, the trend is seen to be similar to that for the theoretical results in Fig. 2 (b). For low SNRs, the scanning result is degraded by the noise of the imaging system, the noise of the detector, disturbances in the light source, and the turbulent atmosphere. With CGI, it is possible to suppress this degradation because by using the correlation method, random noise can be reduced without the need for averaging. This suppression effect indicates a resistance to background noise. Overall, the results show that CGI is useful techniques for various situations.

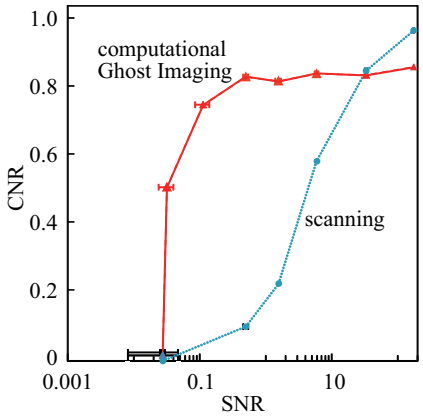

Figure 3. Experimental results of variation of image quality with SNR.

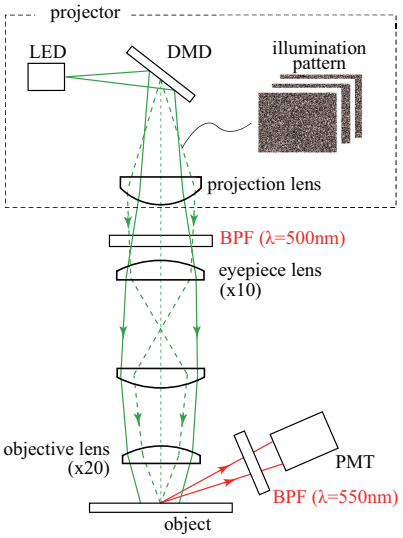

Figure 4. Experimental setup of fluorescent microscope by using the computational GI.

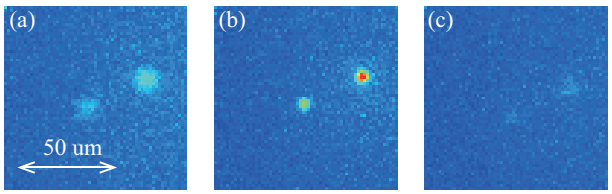

Figure 5. Detected fluorescence images of the calibration slides under various focus conditions. The sample was set at z positions of (a) $+10\mu m$, (b) $0\mu m$ (just focus), and (c) $-10\mu m$.

4 Experimental results

Figure 4 shows an experimental setup of a fluorescent microscope by using the CGI. We have converted a commercial microscope to a CGI microscope by attaching a DMD projector and a bucket detector. The DMD projector(Texas Instruments Inc./ DLP Lightcrafter) and a photomultiplier tube(Hamamatsu Photonics K.K./ H6780-01) as the bucket detector were installed at a eyepiece part of the microscope(Nikon Corp./ ECLIPSE TE200U) and the side of a sample stage, respectively. Random patterns were illuminated onto the sample with an objective lens (x20). For efficiently exciting a sample and detecting an emission light, two band-pass filters (illumination part: 500nm, detected part: 550nm) were placed in front and behind the sample.

Firstly, we have attempted to detect fluorescence images of a calibration slides for basic imaging checks and calibration. In the calibration slides (Polyscience inc., StarLight), there are 6um fluorescent microspheres dyed with Envy Green (the center wavelength of absorption and emission spectrum are 525 and 565 nm, respectively). Figure 5 shows a detected fluorescence images of the calibration slides. Figures 5 (a), (b), and (c) are the focus-shift images using the random patterns illuminated at $z = +10\mu m$, $0\mu m$, and $-10\mu m$, respectively. As shown in fig.5 (b), two fluorescence spheres was detected clearly at the position of the just focus. However, in figs.5 (b) and (c), by shifting the positions of the out of the focus, the detected images were not clear images. Therefore the fluorescence GI microscope has a hight sensitivity and there is possibility to realize a three dimensional imaging.

We have observed a biological sample by the illumination with weak intensity. The sample was human breast cancer cells (MCF) labeled with green fluorescent protein (GFP). Figures 6 (a), (b), and (c) shows fluorescence images detected by using the fluorescence microscope with 9.5 nW/um^2 irradiation, the fluorescence microscope with 150 pW/um^2 irradiation, and the fluorescence CGI microscope to keep irradiating with 150 pW/um^2 after one day, respectively. Image sizes of the each images were 100×100, 100×100, and 100×100 pixels, respectively. Each measurement numbers were 1, 16387×4, and 16387×4, respectively. As shown in fig. 6 (a), the image detected by the normal fluorescence microscope with 19.5 nW/um^2 is clear for observation. However, after 1min illadiation, the fluorescence image could not be detected because of the photobleaching. Although to overcome the photobleaching, excitation power decreased to 150 pW/um^2, the detected image was not clear for observation. On the other hand, by using the fluorescence CGI microscope with 150 pW/um^2 irradiation, the image was clear for observation after one day irradiation as shown in fig.6 (c). By using weak intensity illumination, it is successful for long time

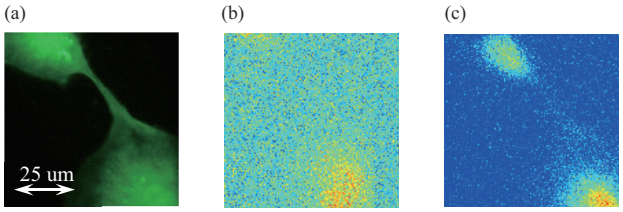

Figure 6. Fluorescence images of MCF-7/GFP cell. (a) fluorescence microscopic image with 9.5 nW/um^2 irradiation, (b) fluorescence microscopic image with 150 pW/um^2 irradiation (number of integration times: 16387 × 4), (c) fluorescence CGI image to keep irradiating with 150 pW/um^2 after one day.

observation against the photo bleaching. For further work, it is necessary to improve a spacial resolution for detailed analysis of biological cells.

5 Conclusions

Fluorescence microscope by using the CGI has been proposed via basic investigations, theoretically and experimentally. In the basic investigations, for detecting the fluorescent light with low SNR condition, the CGI imaging had indicated an advantage compared with the scanning method. The DMD projector was installed into the microscope at the eyepiece and fluorescence light was detected by the photo-multiplier tube. After confirming the depth-dependency, we have detected the fluorescence image from the biological cells for one day without light-induced bleaching.

Acknowledgement

This work was partially supported by MEXT KAKENHI Grant-in-Aid for Exploratory Research 15K13914. Additionally, we wish to thank the timely help given by KURABO Industries ltd. for providing biological samples.

References

[1] J.R. Lakowicz, *Principles of Fluorescence Spectroscopy 3rd edition* (Springer, USA, 1999)
[2] A. Molski, J. Chem. Phys. **114**, 1142 (2001)
[3] S.Nie and R. N. Zare, Annu. Rev. Biophys. Biomol. Struct. **26**, 567 (1997)
[4] A. V. Belinsky and D. N. Klyshko, Sov. Phys. JETP **78**, 259 (1994)
[5] T. B. Pittman, Y. H. Shih, D. V. Strekalov, and A. V. Sergienko, Phys. Rev. A **52**, R3429 (1995).
[6] A. Gatti, E. Brambilla, M. Bache, and L. A. Lugiato, Phys. Rev. Lett. **93**, 093602 (2004).
[7] J. H. Shapiro, Phys. Rev. A **78**, 061802(R) (2008).
[8] B. Sun, M. P. Edgar, R. Bowman, L. E. Vittert, S. Welsh, A. Bowman, and M. J. Padgett, Science. **340**, 844 (2013).
[9] J. D. Winefordner, et al., Spectrochim. Acta. **31 B**, 1 (1976)
[10] G. Scarcelli and S. H. Yun, Opt. Express **16**, 16189 (2008).
[11] N. Tian, Q. Guo, A. Wang, D. Xu, and L. Fu, "Fluorescence ghost imaging with pseudothermal light," Opt. Lett. **36**, 3302 (2011).
[12] M. Tanha, R. Kheradmand, and S. Ahmadi-Kandjani, Appl. Phys. Lett. **101**, 101108 (2012).
[13] M. Tanha, R. Kheradmand, S. Ahmadi-Kandjani, and H. Ghanbari, Eur. Phys. J. D **67**, 1 (2012).
[14] H. Ghanbari-Ghalehjoughi, S. Ahmadi-Kandjani, and M. Eslami, J. Opt. Soc. Am. A **32**, 323 (2015).
[15] K. W. C. Chan, M. N. O'Sullivan, and R. W. Boyd, Opt. Express **18**, 5562 (2010).